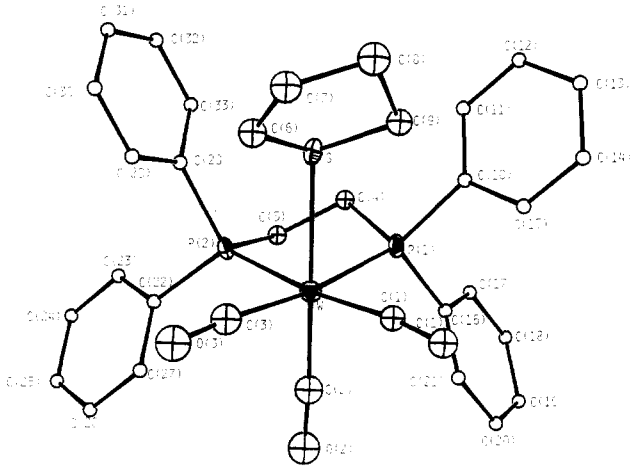

Figure 1. ORTEP drawing of $W(CO)_3(dppe)(2,3\text{-DHT})$ (I).

signals corresponding to 2,3-DHT in I are broadened with no distinct splitting at low temperature (-80 °C). Also, in comparison to the ambient-temperature spectrum, the low-temperature spectra of I show a further upfield shift (~0.2 ppm). However, there are no new signals that may be attributed to a distinctly different coordination mode for 2,3-DHT. Due to the instabilities of I and III over long acquisition times, efforts to obtain evidence for an olefin-coordinated form of 2,3-DHT by the use of $W-^{13}C$ coupling were unsuccessful. Compound I does not react with $[Me_3O]BF_4$; methylation of the sulfur might be expected if 2,3-DHT were coordinated through the olefin.

Other phosphine-substituted 2,3-DHT complexes were prepared in an attempt to understand the observed high-field chemical shifts of the olefinic protons in I. Although trends in their ^1H NMR spectra are not completely understood, it appears that shielding of 2,3-DHT by the phenyl rings of the phosphines in these compounds is primarily responsible for the upfield shifts observed. The solvent also probably plays a role since the 2,3-DHT protons in $W(CO)_5(2,3\text{-DHT})$ are downfield in $CDCl_3$ [δ 6.19 (H(5)), 5.87 (H(4)), 2.96 (H(3)), 3.53 (H(2))] as compared with those in C_6D_6 [δ 5.23 (H(5)), 4.83 (H(4)), 1.87 (H(3)), 2.44 (H(2))].

Acknowledgment. This work was supported by the U.S. Department of Energy under Contract No. W-7405-Eng-82, Office of Basic Energy Sciences, Chemical Sciences and Materials Sciences Divisions.

Registry No. I, 119638-26-5; II, 119638-27-6; III, 119638-28-7; IV, 119638-29-8; V, 119638-30-1; VI, 119638-31-2; VII, 119638-32-3; VIII, 108617-81-8; $W(CO)_4(dppe)$, 29890-05-9; $Mo(CO)_4(dppe)$, 15444-66-3; $W(CO)_4(dmpe)$, 40544-99-8; $W(CO)_5(PPh_3)$, 15444-65-2; $W(CO)_5(PMe_3)$, 26555-11-3; $W(CO)_5(PMePh_2)$, 18534-36-6; $W(CO)_5(PMe_2Ph)$, 42565-94-6.

Supplementary Material Available: Listings of calculated atomic coordinates for hydrogen atoms and all bond angles and distances for $W(CO)_3(dppe)(2,3\text{-DHT})$ (5 pages); a table of calculated and observed structure factors (21 pages). Ordering information is given on any current masthead page.

Contribution from the Department of Chemistry and Laboratory for Molecular Structure and Bonding, Texas A&M University, College Station, Texas 77843

Edge-Sharing Bioctahedral Molecules without Metal-Metal Bonds: The d^6-d^6 Complexes $Rh_2X_4(\mu\text{-}X)_2(\mu\text{-dppm})_2$ (X = Cl, Br)

F. Albert Cotton,* Kim R. Dunbar, Cassandra T. Eagle, Larry R. Falvello, and Andrew C. Price

Received December 20, 1988

There is now a body of structural data for compounds with the edge-sharing bioctahedral structure sufficient to show how bond length and bond order are influenced by various factors, but especially by the d-electron count on each metal atom.[1-3] The influence of electron count alone, other factors being held as constant as possible, has been addressed most effectively by a study of compounds of type I, for which we have examples[2,3] with M = Nb, Ta, Mo, W, Re, and Ru. A less extensive series comprises compounds of type II.[4]

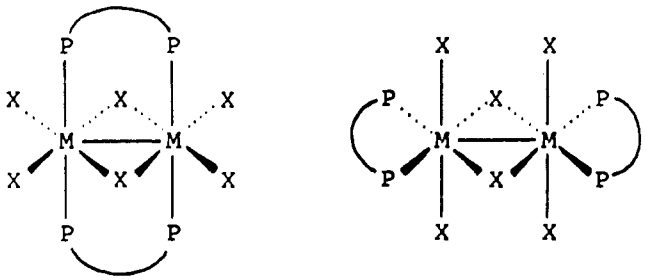

I II

For neither of these series, however, has there been data for a compound with either a d^0 or a d^6 pair of metal atoms, wherein a M-M bond order of 0 would be expected. Our purpose in undertaking the work reported here was to supply such data. We chose the rhodium compounds of type I for three reasons. (1) We felt that without a M-M bond, a type I molecule with its bridging diphosphine ligands would probably be more accessible and stable than one of type II. (2) It seemed that a d^6-d^6 system would be more tractable than a d^0-d^0 system, since Sc^{III}, Y^{III}, and the La^{III} ions are not prone to form bonds to phosphines, whereas rhodium and iridium are. (3) Rhodium seemed a more likely candidate than iridium for many, fairly obvious, reasons.

We first obtained $Rh_2Br_6(dppm)_2$ by chance, but subsequently devised a rational preparation. We include it here for comparison with $Rh_2Cl_6(dppm)_2$ (which was prepared deliberately in the first instance) and with other $M_2Br_6(dppm)_2$ species that we shall report in the future. The preparation and chemical properties of $Rh_2Cl_6(dppm)_2$ have been presented earlier.[5] The preparation of $Rh_2Br_6(dppm)_2$ is described here, and the crystal structures of both compounds are reported.

Experimental Section

The following materials were used as supplied from the indicated sources: $RhBr_3 \cdot 3H_2O$, AESAR, dppm, Aldrich; Br_2, MCB; CO, Matheson. Solvents were freshly distilled from drying agents under dinitrogen prior to use: CH_2Cl_2 from P_2O_5; Et_2O from CaH_2. EtOH (95%) was degassed prior to use. All manipulations, unless otherwise stated, were done under an argon atmosphere by using standard vacuum-line techniques. Infrared spectra were recorded on a Perkin-Elmer 783 spectrophotometer by using Nujol mulls between CsI plates. $^{31}P\{^1H\}$ NMR spectra were recorded on a XL-200 Varian spectrometer at 81 MHz. Chemical shifts were referenced to external 85% H_3PO_4; more positive values represent deshielding.

Preparation of $Rh_2Br_6(dppm)_2$. Method A. This is the method of choice. $[Rh_2(\mu\text{-}Br)(\mu\text{-}CO)(CO)_2(dppm)_2]Br$, 0.152 g, dissolved in 100 mL of CH_2Cl_2 was treated with 10 mL of a Br_2 solution (0.2 g Br_2 in 100 mL of CH_2Cl_2) in a dimly lighted fume hood, or otherwise protected from strong light. The pale yellow-orange solution became cherry red as the Br_2 solution was added gradually over 5 min. After 8 h an additional 10 mL of the stock solution of Br_2 was added. This produced no immediate or marked color change, but after 18 h a solid had precipitated. The solvent was removed under vacuum, leaving 0.180 g (99%) of nearly pure $Rh_2Br_6(dppm)_2$. $^{31}P\{^1H\}$ NMR (CH_2Cl_2): δ = -2.78 ppm, J_{Rh-P} = 85.0 Hz. IR (Nujol, CsI plates): 2720 (w), 1730 (w), 1710 (w),

(1) Cotton, F. A. *Polyhedron* **1987**, *6*, 667 (a comprehensive tabulation to the end of 1986).
(2) Chakravarty, A. R.; Cotton, F. A.; Diebold, M. P.; Lewis, D. B.; Roth, W. J. *J. Am. Chem. Soc.* **1986**, *108*, 971.
(3) Canich, J. A. M.; Cotton, F. A.; Daniels, L. M.; Lewis, D. B. *Inorg. Chem.* **1987**, *26*, 4046.
(4) Agaskar, P. A.; Cotton, F. A.; Dunbar, K. R.; Falvello, L. R.; O'Connor, C. J. *Inorg. Chem.* **1987**, *26*, 4051.
(5) Cotton, F. A.; Eagle, C. T.; Price, A. C. *Inorg. Chem.* **1988**, *27*, 4362.

Table I. Crystal Data for $Rh_2X_6(dppm)_2$ (X = Cl or Br)

compd	$Rh_2Cl_6(dppm)_2 \cdot 3C_6H_6 \cdot 2CH_2Cl_2$	$Rh_2Br_6(dppm)_2 \cdot C_7H_8$
formula	$Rh_2Cl_{10}P_4C_{70}H_{66}$	$Rh_2Br_6P_4C_{57}H_{52}$
fw	1591.53	1546.17
space group	$P\bar{1}$	$P\bar{1}$
a, Å	9.809 (3)	12.198 (6)
b, Å	12.130 (4)	15.974 (8)
c, Å	16.289 (7)	10.061 (4)
α, deg	94.42 (3)	99.62 (1)
β, deg	101.80 (3)	108.42 (1)
γ, deg	108.69 (3)	80.40 (1)
V, Å^3	1776 (1)	1820 (3)
Z	1	1
d_{calcd}, g/cm^3	1.112	1.410
μ(Mo Kα), cm^{-1}	7.991	76.47
radiation (monochromated in incident beam)	Mo Kα (λ_α = 0.710 73 Å)	
temp, °C	22 ± 2	22 ± 2
transmissn factors: max, min	99.73, 83.64	99.79, 87.90
R^a	0.0395	0.0684
R_w^b	0.0522	0.0972

$^a R = \sum||F_o| - |F_c||/\sum|F_o|$. $^b R_w = [\sum w(|F_o| - |F_c|)^2/\sum w|F_o|^2]^{1/2}$; $w = 1/\sigma^2(|F_o|)$.

Table II. Selected Bond Distances (Å) and Angles (deg) for $Rh_2Cl_6(dppm)_2$ and $Rh_2Br_6(dppm)_2$[a]

$Rh_2Cl_6(dppm)_2$		$Rh_2Br_6(dppm)_2$	
Distances			
Rh(1)–Rh(1)′	3.425 (1)	Rh(1)–Rh(1)′	3.522 (3)
Rh(1)–Cl(1)	2.375 (1)	Rh(1)–Br(1)	2.491 (4)
Rh(1)–Cl(1)′	2.369 (1)	Rh(1)–Br(1)′	2.488 (4)
Rh(1)–Cl(2)	2.311 (1)	Rh(1)–Br(2)	2.447 (5)
Rh(1)–Cl(3)	2.306 (2)	Rh(1)–Br(3)	2.457 (4)
Rh(1)–P(1)	2.368 (1)	Rh(1)–P(1)	2.391 (8)
Rh(1)–P(2)	2.399 (2)	Rh(1)–P(2)	2.399 (8)
P(1)–C(1)	1.860 (5)	P(1)–C(1)	1.89 (2)
P(1)–C(2)	1.831 (5)	P(1)–C(2)	1.83 (3)
P(1)–C(8)	1.823 (5)	P(1)–C(8)	1.85 (3)
P(2)–C(1)′	1.847 (4)	P(2)–C(1)′	1.82 (3)
P(2)–C(14)	1.826 (5)	P(2)–C(14)	1.88 (3)
P(2)–C(20)	1.803 (6)	P(2)–C(20)	1.79 (2)
Angles			
Rh(1)–Cl(1)–Rh(1)′	92.43 (4)	Rh(1)–Br(1)–Rh(1)′	90.1 (2)
Cl(1)–Rh(1)–Cl(1)′	87.57 (4)	Br(1)–Rh(1)–Br(1)′	89.9 (1)
Cl(1)–Rh(1)–Cl(2)	89.86 (5)	Br(1)–Rh(1)–Br(2)	90.6 (2)
Cl(1)–Rh(1)–Cl(3)	177.34 (5)	Br(1)–Rh(1)–Br(3)	178.7 (2)
Cl(2)–Rh(1)–Cl(3)	90.12 (5)	Br(2)–Rh(1)–Br(3)	90.5 (1)
Cl(1)–Rh(1)–P(1)	86.40 (4)	Br(1)–Rh(1)–P(1)	88.6 (2)
Cl(1)–Rh(1)–P(2)	87.99 (4)	Br(1)–Rh(1)–P(2)	85.7 (2)
P(1)–Rh(1)–P(2)	173.88 (4)	P(1)–Rh(1)–P(2)	172.4 (3)
Rh(1)–P(1)–C(1)	111.0 (2)	Rh(1)–P(1)–C(1)	112.1 (8)
Rh(1)–P(2)–C(1)′	111.4 (2)	Rh(1)–P(2)–C(1)′	112.5 (8)
P(1)–C(1)–P(2)′	118.6 (3)	P(1)–C(1)–P(2)′	119.0 (2)

[a] Numbers in parentheses are estimated standard deviations in the least significant digits.

1590 (w), 1575 (w), 1435 (s), 1310 (w), 1265 (m), 1195 (w), 1165 (w), 1135 (w), 1100 (m), 1040 (w), 1010 (w), 810 (m), 775 (s), 740 (s), 710 (m), 695 (s), 530 (s), 520 (m), 495 (m), 465 (w), 405 (w), 380 (w) cm^{-1}.

The starting material, $[Rh_2(\mu\text{-Br})(\mu\text{-CO})(CO)_2(dppm)_2]Br$, may be made by halide exchange on $Rh_2(CO)_2Cl_2(dppm)_2$ according to Cowie and Dwight[6] or by the following procedure. A solution of $RhBr_3 \cdot 3H_2O$ (0.934 g) in 100 mL of 95% ethanol was heated to 75 °C, and CO was bubbled through the solution for 2 h. This yellow-orange solution was evaporated to dryness, and the light brown solid was treated with 20 mL of CH_2Cl_2 to form a slurry. A solution of 0.905 g of dppm in 20 mL of CH_2Cl_2 was added, and a clear orange solution was formed within 30 min. This solution was concentrated to 5 mL, and 20 mL of Et_2O was added to precipitate an orange-yellow powder, which was separated by filtration, washed with Et_2O (3 × 10 mL), and dried with an aspirator pump. Yield: 1.25 g, 87%. IR (CO region, mineral oil mull): 2110 (m), 1965 (s), 1860 (m) cm^{-1}. $^{31}P\{^1H\}$ NMR (CH_2Cl_2): δ = −29.8 ppm, J_{Rh-P} = 94.1 Hz.

Method B. This was the method first used and provided the crystal used for X-ray work. Anhydrous $Rh_2(O_2CCH_3)_4$ (50 mg, 0.11 mmol), dppm (90 mg, 0.23 mmol), and Me_3SiBr (65 mL, 0.49 mmol) were added to a Schlenk flask containing 20 mL of freshly distilled toluene. The mixture was stirred at ambient temperature under argon for 14 h, during which time the green suspension of $Rh_2(O_2CCH_3)_4$ was gradually replaced by a pale orange precipitate and an orange-brown solution. After the solids had been removed by suction filtration, the filtrate was allowed to evaporate slowly in air. A crop of red crystals was obtained after 1 week. Yield: 10 mg, ~6%.

X-ray Crystallography. The structures of both molecules were determined by general procedures fully described elsewhere.[7] Data reductions were carried out by standard methods using well-established

Table III. Positional Parameters and Equivalent Isotropic Thermal Parameters and Their Estimated Standard Deviations for $Rh_2Cl_6(dppm)_2 \cdot 3C_6H_6 \cdot 2CH_2Cl_2$

atom	x	y	z	B, Å^2[a]
Rh(1)	−0.60026 (4)	−0.64778 (3)	0.47645 (2)	2.04 (1)
Cl(1)	−0.3657 (1)	−0.5270 (1)	0.56398 (7)	2.38 (3)
Cl(2)	−0.8314 (1)	−0.7576 (1)	0.39079 (9)	3.46 (3)
Cl(3)	−0.5681 (2)	−0.8178 (1)	0.51675 (9)	3.22 (3)
P(1)	−0.6969 (1)	−0.6239 (1)	0.59592 (8)	2.23 (3)
P(2)	−0.4811 (1)	−0.6527 (1)	0.36209 (8)	2.36 (3)
C(1)	−0.6967 (5)	−0.4710 (4)	0.6178 (3)	2.4 (1)
C(2)	−0.6117 (6)	−0.6534 (5)	0.6990 (3)	3.0 (1)
C(3)	−0.4826 (6)	−0.6804 (5)	0.7146 (4)	3.5 (2)
C(4)	−0.4255 (8)	−0.7014 (6)	0.7942 (4)	4.7 (2)
C(5)	−0.496 (1)	−0.6954 (7)	0.8583 (5)	6.1 (3)
C(6)	−0.621 (1)	−0.670 (1)	0.8415 (5)	8.7 (4)
C(7)	−0.678 (1)	−0.6469 (9)	0.7651 (5)	6.5 (3)
C(8)	−0.8911 (5)	−0.7119 (4)	0.5843 (3)	2.6 (1)
C(9)	−0.9245 (6)	−0.8334 (5)	0.5777 (4)	3.6 (2)
C(10)	−1.0687 (7)	−0.9080 (5)	0.5708 (4)	4.1 (2)
C(11)	−1.1805 (6)	−0.8611 (6)	0.5696 (4)	4.2 (2)
C(12)	−1.1492 (6)	−0.7423 (5)	0.5739 (4)	4.1 (2)
C(13)	−1.0053 (6)	−0.6672 (5)	0.5815 (4)	3.2 (1)
C(14)	−0.5699 (5)	−0.6503 (5)	0.2524 (3)	2.9 (1)
C(15)	−0.6988 (6)	−0.6256 (5)	0.2288 (4)	3.5 (2)
C(16)	−0.7563 (7)	−0.6204 (7)	0.1451 (4)	4.8 (2)
C(17)	−0.6871 (8)	−0.6426 (7)	0.0838 (4)	5.4 (2)
C(18)	−0.5604 (9)	−0.6679 (8)	0.1061 (4)	6.4 (3)
C(19)	−0.5015 (7)	−0.6729 (7)	0.1889 (4)	5.2 (2)
C(20)	−0.4247 (6)	−0.7795 (4)	0.3497 (3)	2.8 (1)
C(21)	−0.2797 (6)	−0.7773 (5)	0.3632 (4)	3.3 (1)
C(22)	−0.2488 (7)	−0.8798 (5)	0.3500 (4)	4.0 (2)
C(23)	−0.3613 (8)	−0.9860 (5)	0.3248 (4)	4.3 (2)
C(24)	−0.5054 (7)	−0.9907 (5)	0.3128 (5)	4.6 (2)
C(25)	−0.5370 (6)	−0.8900 (5)	0.3251 (4)	4.1 (2)
C(26)[b]	−1.048 (1)	−0.591 (1)	0.2299 (8)	9.1 (5)
C(27)[b]	−1.019 (1)	−0.489 (1)	0.1989 (9)	9.3 (5)
C(28)[b]	−1.073 (1)	−0.486 (1)	0.116 (1)	9.1 (4)
C(29)[b]	−1.150 (1)	−0.584 (1)	0.0628 (8)	9.0 (4)
C(30)[b]	−1.184 (1)	−0.686 (1)	0.0883 (9)	8.8 (4)
C(31)[b]	−1.134 (1)	−0.697 (1)	0.172 (1)	9.6 (5)
C(32)[b]	−0.385 (2)	−0.046 (1)	0.014 (1)	12.0 (7)
C(33)[b]	−0.438 (2)	−0.015 (1)	0.0774 (9)	10.6 (6)
C(34)[b]	−0.544 (3)	0.030 (1)	0.067 (1)	11.8 (7)
C,Cl(35)[b,c]	−0.967 (2)	−0.061 (2)	−0.7893 (9)	26 (2)
C,Cl(36)[b,c]	−0.956 (2)	0.050 (1)	−0.8219 (9)	15.7 (6)
C,Cl(37)[b,d]	−0.926 (3)	0.001 (2)	−0.899 (2)	48 (2)
C,Cl(38)[b,e]	−0.972 (3)	−0.127 (2)	−0.925 (1)	36 (2)
C,Cl(39)[b,d]	−0.917 (2)	−0.1417 (9)	−0.837 (1)	18.8 (7)
Cl(9)[b,f]	−1.095 (2)	−0.022 (2)	−0.805 (1)	17.3 (9)

[a] B values for anisotropically refined atoms are given in the form of the equivalent isotropic displacement parameter defined as $(1/3)[a^2a^{*2}B_{11} + b^2b^{*2}B_{22} + c^2c^{*2}B_{33} + 2ab(\cos\gamma)a^*b^*B_{12} + 2ac(\cos\beta)a^*c^*B_{13} + 2bc(\cos\alpha)b^*c^*B_{23}]$. [b] Estimated standard deviations for these sites are taken from the last cycle in which the parameters of the sites were refined. [c] Site modeled as $^2/_7$ C + $^2/_7$ Cl. [d] Site modeled as $^1/_7$ C + $^3/_7$ Cl. [e] Site modeled as $^1/_7$ C + $^2/_7$ Cl. [f] Site modeled as $^2/_7$ Cl.

(6) Cowie, M.; Dwight, S. K. *Inorg. Chem.* **1980**, *19*, 2500.

(7) (a) Bino, A.; Cotton, F. A.; Fanwick, P. E. *Inorg. Chem.* **1979**, *18*, 3558. (b) Cotton, F. A.; Frenz, B. A.; Deganello, G.; Shaver, A. *J. Organomet. Chem.* **1973**, *50*, 227.

Table IV. Positional Parameters and Equivalent Isotropic Thermal Parameters and Their Estimated Standard Deviations for $Rh_2Br_6(dppm)_2 \cdot C_7H_8$

atom	x	y	z	B, Å^{2a}
Rh(1)	0.6498 (2)	0.4749 (2)	0.5834 (3)	2.66 (5)
Br(1)	0.5322 (2)	0.5660 (2)	0.3972 (3)	3.05 (7)
Br(2)	0.8296 (3)	0.5166 (2)	0.5695 (3)	3.95 (8)
Br(3)	0.7621 (3)	0.3854 (2)	0.7693 (3)	4.01 (8)
P(1)	0.3576 (7)	0.6446 (5)	0.5961 (8)	3.3 (2)
P(2)	0.6303 (6)	0.5998 (5)	0.7476 (8)	3.1 (2)
C(1)	0.483 (2)	0.626 (2)	0.761 (2)	2.0 (5)^b
C(2)	0.369 (2)	0.753 (2)	0.569 (3)	3.5 (8)
C(3)	0.394 (2)	0.773 (2)	0.460 (3)	3.9 (8)
C(4)	0.401 (3)	0.862 (2)	0.450 (3)	4.7 (9)
C(5)	0.391 (3)	0.922 (2)	0.549 (4)	7 (1)
C(6)	0.370 (4)	0.902 (2)	0.673 (4)	11 (2)
C(7)	0.351 (4)	0.818 (2)	0.677 (4)	8 (1)
C(8)	0.232 (2)	0.661 (2)	0.667 (3)	4.2 (9)
C(9)	0.126 (2)	0.689 (2)	0.557 (3)	6 (1)
C(10)	0.028 (4)	0.703 (2)	0.597 (3)	8 (1)
C(11)	0.030 (3)	0.687 (2)	0.739 (4)	6 (1)
C(12)	0.135 (2)	0.658 (2)	0.848 (4)	7 (1)
C(13)	0.238 (2)	0.644 (2)	0.800 (3)	4.5 (9)
C(14)	0.664 (2)	0.707 (2)	0.728 (3)	4.3 (9)
C(15)	0.691 (2)	0.722 (2)	0.609 (3)	3.7 (7)
C(16)	0.716 (2)	0.799 (2)	0.593 (3)	5.1 (9)
C(17)	0.709 (4)	0.861 (3)	0.693 (5)	10 (1)^b
C(18)	0.664 (5)	0.863 (4)	0.822 (6)	17 (2)^b
C(19)	0.663 (4)	0.766 (3)	0.845 (5)	12 (2)
C(20)	0.716 (2)	0.586 (2)	0.925 (2)	2.7 (7)
C(21)	0.669 (2)	0.573 (2)	1.026 (3)	3.7 (8)
C(22)	0.743 (3)	0.564 (2)	1.170 (3)	5.2 (9)
C(23)	0.868 (3)	0.564 (2)	1.193 (4)	7 (1)
C(24)	0.919 (3)	0.576 (3)	1.088 (3)	7 (1)
C(25)	0.839 (2)	0.586 (2)	0.955 (3)	5.2 (9)
C(26)	0.283 (6)	0.876 (5)	−0.002 (8)	22 (3)^b
C(27)	0.352 (4)	0.804 (3)	0.062 (5)	10 (1)^b
C(28)	0.409 (3)	0.898 (3)	0.060 (4)	8 (1)^b
C(29)	0.505 (4)	0.899 (3)	0.116 (5)	10 (1)^b
C(30)	0.587 (4)	0.833 (4)	0.177 (6)	13 (2)^b
C(31)	0.540 (4)	0.758 (3)	0.170 (5)	10 (1)^b
C(32)	0.436 (3)	0.751 (3)	0.124 (4)	8 (1)^b

^{a} *B* values for anisotropically refined atoms are given in the form of the equivalent isotropic displacement parameter defined as $(1/3)[a^2a^{*2}B_{11} + b^2b^{*2}B_{22} + c^2c^{*2}B_{33} + 2ab(\cos\gamma)a^*b^*B_{12} + 2ac(\cos\beta)a^*c^*B_{13} + 2bc(\cos\alpha)b^*c^*B_{23}]$. ^{b} Atoms were refined isotropically.

computational procedures.[8] The crystal parameters and basic information pertaining to data collection and structure refinement are summarized in Table I. Selected bond distances and bond angles for both compounds are found in Table II, while positional parameters for both structures are given in Tables III and IV. Complete tables of crystal, data collection, and structure refinement parameters, bond distances and angles, anisotropic thermal parameters, and structure factors are available as supplementary material.

Both the Patterson peak search and the direct-methods program in SHELXS–86[9] led to the location of the Rh atoms in both compounds. A sequence of successive difference Fourier maps and least-squares cycles led to full development of the coordination spheres. For $Rh_2Cl_6(dppm)_2$, one interstitial disordered dichloromethane molecule lying on a general position, one benzene molecule lying on a general position, and one benzene molecule lying on a special position (giving a total of three benzenes) were located and refined. Anisotropic refinement was successfully completed to give $R = 0.0395$ and $R_w = 0.0522$, using 4211 reflections to fit 505 variables. A detailed account of how the interstitial solvent molecules were refined may be found in the supplementary material.

For $Rh_2Br_6(dppm)_2$, one toluene molecule per rhodium dimer was located. After isotropic convergence was achieved, the absorption correction DIFABS was applied.[10] Anisotropic refinement gave $R = 0.0684$ and $R_w = 0.0972$, using 2195 reflections to fit 293 variables.

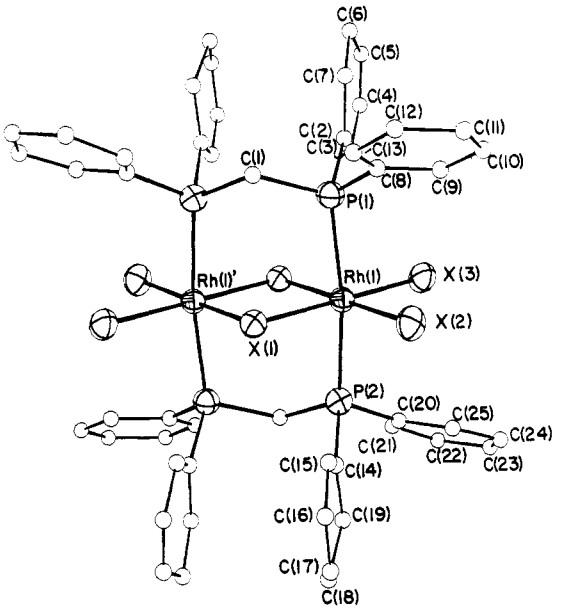

Figure 1. ORTEP diagram of $Rh_2X_6(dppm)_2$ (X = Cl or Br), showing the atom-labeling scheme. The phenyl carbon atoms are shown as small circles for clarity. All other atoms are represented by their 40% probability ellipsoids.

Table V. List of Edge-Sharing Bioctahedral Complexes

complex	M–M dist, Å	electronic confign	bond order	ref
$Nb_2Cl_6(dmpm)_2$	2.711 (3)	$\sigma^2\pi^2$	2	11
$Ta_2Cl_6(dmpm)_2$	2.692 (2)	$\sigma^2\pi^2$	2	2
$Mo_2Cl_6(dmpm)_2$	2.7394 (5)	$\sigma^2\pi^2\delta^{*2}$	1	3
$Mo_2Cl_6(dppm)_2$	2.789 (1)	$\sigma^2\pi^2\delta^{*2}$	1	2
$W_2Cl_6(dmpm)_2$	2.6663 (4)	$\sigma^2\pi^2\delta^{*2}$	1	3
$W_2Cl_6(dppm)_2$	2.691 (1)	$\sigma^2\pi^2\delta^{*2}$	1	3
$Re_2Cl_6(dmpm)_2$	2.5807 (4)	$\sigma^2\pi^2\delta^{*2}\delta^2$	2	3
$Re_2Cl_6(dppm)_2$	2.616 (1)	$\sigma^2\pi^2\delta^{*2}\delta^2$	2	12
$Ru_2Cl_6(dmpm)_2$	2.933 (1)	$\sigma^2\pi^2(\delta\delta^*)^4\pi^{*2}$	1	2
$Rh_2Cl_6(dppm)_2$	3.425 (1)	$\sigma^2\pi^2(\delta\delta^*)^4\pi^{*2}\sigma^{*2}$	0	this work
$Rh_2Br_6(dppm)_2$	3.522 (3)	$\sigma^2\pi^2(\delta\delta^*)^4\pi^{*2}\sigma^{*2}$	0	this work
$Rh_2Cl_6(P\text{-}n\text{-}Bu_3)_4$	3.745 (15)	$\sigma^2\pi^2(\delta\delta^*)^4\pi^{*2}\sigma^{*2}$	0	13

Results and Discussion

The title compounds, $Rh_2Cl_6(dppm)_2$ and $Rh_2Br_6(dppm)_2$, may be prepared in high yield from $Rh_2(CO)_2Cl_2(dppm)_2$ and $[Rh_2(CO)_3Br(dppm)_2]Br$, respectively, with the appropriate halogen under mild conditions. Both complexes are air-stable, but the crystals tend to loose solvent rapidly. Their $^{31}P\{^1H\}$ NMR spectra display an AX pattern centered at $\delta = 4.65$ (X = Cl) and $\delta = -2.78$ (X = Br), which is consistent with their solid-state structures. An ORTEP diagram is shown in Figure 1.

The most important results of this study, by far, are the distances between the pairs of rhodium atoms and how they compare with those in other related dimetal systems possessing the edge-sharing bioctahedral structure of type I. A complete list of compounds having this structure, their M–M separations, electronic configurations, and bond orders is shown in Table V. In addition, we have included another d^6–d^6 dirhodium complex, $Rh_2Cl_6(P\text{-}n\text{-}Bu_3)_4$,[13] for comparison. Note that in the case of the Rh–Rh complexes, it is impossible to infer whether the δ orbital lies above or below the δ^* orbital, but, of course, it is not critical to do so, since both are filled.

An extensive comparison of most of these structures has already been given elsewhere,[3] but there are a few additional points worthy of note. In going from the Re to the Ru compound with the same

(8) Crystallographic computing was done on a Local Area VAX Cluster, employing the VAX/VMS V4.6 computer.
(9) Sheldrick, G. M. "SHELXS-86"; Institute for Anorganische Chemie der Universitat, Göttingen, FRG, 1986.
(10) Walker, N.; Stuart, D. *Acta Crystallogr.* **1983**, *A39*, 158.
(11) Cotton, F. A.; Duraj, S. A.; Falvello, L. R.; Roth, W. J. *Inorg. Chem.* **1985**, *24*, 4389.
(12) Barder, T. J.; Cotton, F. A.; Lewis, D.; Schwotzer, W.; Tetrick, S. M.; Walton, R. A. *J. Am. Chem. Soc.* **1984**, *106*, 2882.
(13) Muir, J. A.; Muir, M. M.; Rivera, A. J. *Acta Crystallogr.* **1974**, *B30*, 2062.

Table VI. Bond Length Comparisons Showing the Effect of Buttressing Ligands[a]

metal	M–M bond dist, Å				
	buttressed		unbuttressed		diff
Nb	$Nb_2Cl_6(dmpm)_2$	2.711 (3)	$Nb_2Cl_6(dppe)_2$	2.729 (2)	~0
			$Nb_2Cl_6(dppm)_2$	2.696 (1)	
Ta	$TaCl_6(dmpm)_2$	2.692 (2)	$Ta_2Cl_6(PMe_3)_4$	2.721 (1)	~0.02
			$Ta_2Cl_6(dmpe)_2$	2.710 (1)	
Mo	$Mo_2Cl_6(dppm)_2$	2.789 (1)	$Mo_2Cl_6(depe)_2$	2.785 (3)[b]	~0
			$Mo_2Cl_6(dppe)_2$	2.762 (1)[b]	
W	$W_2Cl_6(dppm)_2$	2.691 (1)[c]	$W_2Cl_6(PMe_3)_4$	2.711 (1)[d]	0.02
Re	$Re_2Cl_6(dppm)_2$	2.667 (1)	$Re_2Cl_6(dppe)_2$	3.809 (1)	1.14
Ru	$Ru_2Cl_6(dmpm)_2$	2.933 (1)[e]	$Ru_2Cl_6(PBu_3)_4$	3.733 (2)[f]	0.80

[a] Unreferenced data are found in ref 1. A few other compounds might have been included but would not change the picture. [b] Reference 4. [c] Reference 3. [d] Chisholm, M. H. private communication. [e] This compound is listed in the table in ref 1 but mistakenly shown as $Ru_2Cl_6(dppm)_2$. [f] Cotton, F. A.; Matusz, M.; Torralba, R. C. *Inorg. Chem.* **1989**, *28*, 1516.

ligand in each (dmpm), there is an increase of 0.35 Å, attributable to the loss of the π component of M–M bonding. We cannot directly compare Ru and Rh compounds with the same ligand, but it is probably safe to do so indirectly by noting that, for Mo, W, and Re, the change from dmpm to dppm ligands causes an increase of ca. 0.04 Å in the M–M distances. We might thus estimate that, for the $Ru_2Cl_6(dppm)_2$ molecule, the Ru–Ru distance would be 2.93 + 0.04 = 2.97 Å. Thus, on loss of the σ bond as we go from $Ru_2Cl_6(dppm)_2$ to $Rh_2Cl_6(dppm)_2$, the increase is ca. 0.45 Å. This greater increase presumably reflects the greater strength of the σ bond compared to the π bond.

Comparison of the Rh–Rh distances in $Rh_2Cl_6(dppm)_2$ and $Rh_2Br_6(dppm)_2$ shows that the expected effect of increasing the size of the bridging atoms translates into an approximately 0.10-Å increase in the metal–metal distance for this type of compound. Whether this number will be, approximately, valid more generally remains to be seen. No other such direct comparison seems yet to have been reported.[1]

Finally, the increase in Rh–Rh distance from the buttressed case of $Rh_2Cl_6(dppm)_2$ to the unbuttressed case of $Rh_2Cl_6(PBu_3)_4$ of about 0.3 Å invites comparison with similar pairs of compounds formed by M(III) metal atoms where, unlike the Rh case, M–M bonding occurs—or can occur. Pertinent data are gathered in Table VI. Clearly, in cases where there are d^2 and d^3 M(III) atoms, which form bonds of order 2, the buttressing effect is not seen. Presumably in these cases the drive to form M–M bonds is so strong, and the bonds formed are intrinsically so short (2.68–2.78 Å), that the buttressing ligands, dmpm and dppm, do little to affect them. When we reach the d^4–d^4 case, as exemplified by Re(III), there is clearly an enormous change. Here, in the absence of the buttressing type of ligand no M–M bond formation occurs at all (Re···Re = 3.81 Å), while the use of a buttressing ligand leads to M–M bond formation and indeed to the formation of a very strong, short (2.67 Å) bond of order 2.

It is *not* evident why this discontinuous change in behavior occurs, but it *is* evident that the pattern persists as we go to the d^5–d^5 case as exemplified by Ru(III). Here again, in the absence of the buttressing effect, there is no M–M bond (Ru···Ru = 3.73 Å) whereas when two of the dmpm buttressing ligands are present, a net single bond (2.93 Å) is formed.

In the case of d^6–d^6 exemplified by Rh(III), there is no M–M bond formed under any circumstances, as expected. The 0.3-Å shortening caused by the use of buttressing ligands shows that a "buttressing effect", when not covered up or overwhelmed by any other effect (e.g., M–M bonding), can be appreciable when the M···M distances are large (ca. 3.5 Å) but still not nearly capable of drawing the M atoms as close together as they are drawn by even a single bond (i.e., <3.0 Å in the Ru(III) case).

Acknowledgment. We are grateful to the National Science Foundation for support, and we thank F. L. Campbell, III, for assistance.

Supplementary Material Available: For both crystal structures, full tables of crystal parameters and details of data collection and refinement, bond distances, bond angles, and anisotropic displacement parameters and, for $Rh_2Cl_6(dppm)_2 \cdot 3C_6H_6 \cdot 2CH_2Cl_2$, a table of H atom coordinates with isotropic displacement parameters and a detailed account of how the interstitial solvent molecules were refined (15 pages); tables of observed and calculated structure factors (36 pages). Ordering information is given on any current masthead page.

Contribution from the Institut für Physikalische und Theoretische Chemie and Physikalisches Institut, Abt. II, University of Erlangen-Nürnberg, D-8520 Erlangen, West Germany, and Laboratoire de Spectrochimie des Eléments de Transition, Université de Paris-Sud, F-91405 Orsay, France

X-ray Powder Diffraction at the Spin-State Transition in [*N*,*N*′-Ethylenebis(3-carboxysalicylaldiminato)]cobalt(II) Complexes

E. König,*[1a] G. Ritter,[1b] J. Dengler,[1b] P. Thuéry,[2] and J. Zarembowitch*[2]

Received June 29, 1988

Although thermally induced spin-state transitions may arise for compounds of transition metals with electronic configurations d^4, d^5, d^6, d^7, and d^8, most experimental studies have been confined to those of iron(II), iron(III), and cobalt(II).[3-5] Two different types of transition may be readily distinguished: (i) discontinuous transitions, which are characterized by an abrupt change of the relevant physical properties, thus defining the transition temperature, T_c; (ii) continuous transitions, which show a gradual variation of the physical properties over an extended range of temperature (T_c being defined by the temperature where the high-spin fraction $n_{HS} = 0.50$).[4] Spin-state transitions are accompanied by a significant modification of molecular geometry, the most remarkable being the variation in the metal–donor atom distance.[6] The coordination sphere volume becomes smaller on passing from the high-spin (HS) to the low-spin (LS) state, which generally results in a lowering of the molecular volume.

For a number of iron(II) spin transition systems, it has been shown[4] that a clear distinction between the two types of transition may be achieved by the study of X-ray powder diffraction over a range of temperatures inclusive of T_c. For discontinuous transitions, distinct and individual X-ray diffraction patterns for the two spin states, HS and LS, are observed. In the transition region, these patterns replace each other as the transition progresses in either direction, one diminishing while the other gains in intensity. The temperature dependence of the relative intensity I_{HS}/I_{tot} conforms to the temperature variation of n_{HS} as determined from, for example, the temperature dependence of magnetism. For continuous transitions a single X-ray diffraction pattern is in general encountered, the Bragg angle for any particular line displaying a continuous shift in the transition region. This shift is a consequence of the variation in unit cell volume and the associated change of lattice parameters in the course of the LS $\rightleftharpoons$ HS transition and thus exceeds by far the normal temperature shift of the reflections.

It is of interest to determine whether results analogous to those for iron(II) complexes can be established for spin-state transitions of other transition-metal ions. In this paper, we report, therefore, the first study of high-resolution X-ray powder diffraction in the spin-transition region for cobalt(II) complexes. The two six-coordinate compounds chosen are $Co(H_2fsa_2en)(py)_2$ (A) and Co-

(1) (a) Institut für Physikalische und Theoretische Chemie, University of Erlangen-Nürnberg. (b) Physikalisches Institut, Abt. II, University of Erlangen-Nürnberg.
(2) Laboratoire de Spectrochimie des Eléments de Transition, Université de Paris-Sud.
(3) Gütlich, P. *Struct. Bonding* **1981**, *44*, 83.
(4) König, E.; Ritter, G.; Kulshreshtha, S. K. *Chem. Rev.* **1985**, *85*, 219.
(5) Martin, R. L.; White, A. H. *Transition Met. Chem. (N.Y.)* **1968**, *4*, 113.
(6) König, E. *Prog. Inorg. Chem.* **1987**, *35*, 527.

0020-1669/89/1328-1757$01.50/0